

Quantum Monte-Carlo study of magnetic ordering in ZnV_2O_4

Yasuyuki Kato

*Theoretical division and Center for Nonlinear Studies,
Los Alamos National Lab, Los Alamos NM 87545 USA*

(Dated: February 27, 2012)

Abstract

We study the magnetic ordering of Vanadium spinels by Quantum Monte Carlo simulations of a three-band Hubbard model. Vanadium spinels, AV_2O_4 , exhibit a unique “up-up-down-down” spin ordering at low temperatures. While this magnetic ordering was originally measured in 1973, its origin has remained unclear for many years due to the lack of unbiased approaches for solving the relevant model. A three-band Hubbard model on the spinel lattice (corner sharing tetrahedra) is a minimal Hamiltonian for describing the t_{2g} electrons of the V^{2+} ions. One of the main difficulties is that this family of compounds belongs to the elusive intermediate-coupling regime ($U \gtrsim t$) for which there is no small parameter that can justify a perturbative expansion. We present a controlled Quantum Monte-Carlo approach to the three-band Hubbard model relevant for this materials that reproduces the up-up-down-down spin ordering. The method is free of the sign problem that is usually the main limiting factor for simulating fermionic systems in dimension higher than one.

PACS numbers:

I. INTRODUCTION

Interacting electrons in crystals exhibit a variety of cooperative phenomena. This is particularly evident for Mott insulators whose valence electrons are localized due to a rather strong intra-orbital Coulomb repulsion. The degree of electronic localization is controlled by the ratio U/t , where t is the dominant transfer integral between different atomic orbitals. The strong ($U/t \gg 1$) and weak-localization ($t/U \ll 1$) regimes can be treated by expanding in the small parameters t/U or U/t . Unfortunately, this is not true for the intermediate-coupling regime ($U/t \gtrsim 1$) because of the lack of small parameter. Therefore, it is very important to develop controlled and unbiased numerical techniques that can address this elusive regime. The main obstacle for Monte Carlo simulations is the sign problem that can arise from the fermionic statistics of the electronic degrees of freedom or the frustrated nature of the Hamiltonian terms.

In this paper, we focus on the Vanadium spinels $A^{2+}V_2^{3+}O_4^{2-}$, a class of highly frustrated Mott insulators that belong to the intermediate-coupling regime. These systems comprise a pyrochlore lattice (corner sharing tetrahedra) of V^{3+} ions (see Fig. 1(a)). Each V^{3+} ion has two in 3- d electrons in the t_{2g} orbitals, while the O^{2-} and Zn^{2+} ions are in closed shell configurations. Consequently, the low-energy electronic spectrum consists of spin and orbital excitations that arise from the localized 3- d electrons in the V^{3+} ions.

The lattice symmetry of AV_2O_4 is cubic ($Fd\bar{3}m$) at high temperatures. The crystal field produced by the octahedral coordination of O^{2-} ions splits the V^{3+} 3 d -orbitals into high-energy e_g and low-energy t_{2g} orbitals. ZnV_2O_4 undergoes a structural cubic to tetragonal ($I4_1/amd$) transition at $T = 45 \sim 51(K)$ [1, 2]. This structural transition causes further crystal field splitting of the t_{2g} orbitals into xy -orbital and yz, zx -orbitals. (See Fig.1(c).) A magnetic transition to *up-up-down-down* magnetic ordering (uudd-MO) occurs at a lower temperature $T_N = 31 \sim 40(K)$ [1, 2]. The magnetic ordering has a period of 4 lattice sites ($\cdots \uparrow\uparrow\downarrow\downarrow \cdots$) for chains oriented along the yz ($0, \pm 1, \pm 1$) and zx ($\pm 1, 0, \pm 1$) directions. The origin of the uudd-MO and the lack of orbital ordering in this material have been an open this magnetic ordering was originally reported in 1973 [3]. More recent measurements of the pressure dependence of T_N in different spinel vanadates [4] indicate that ZnV_2O_4 belongs to the intermediate-coupling regime: T_N decreases with pressure instead of increasing according to the Bloch's law [5] that is expected for the strong-coupling regime. Previous attempts

at explaining these properties were based on strong-coupling [6–9] or weak-coupling expansions [10] whose validity is not guaranteed for the intermediate-coupling regime relevant for ZnV_2O_4 .

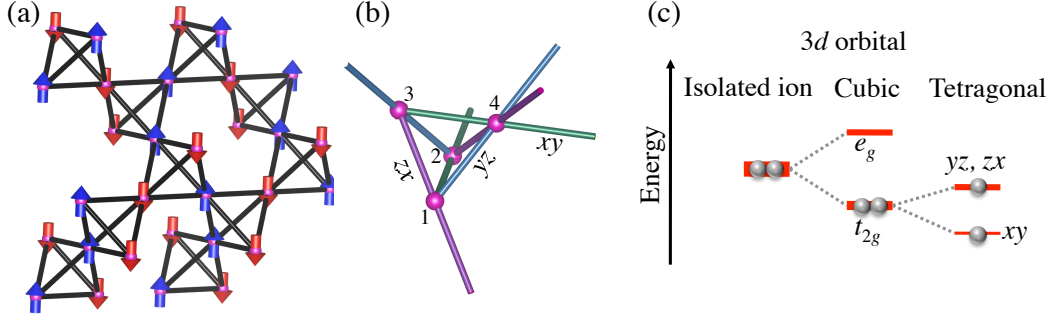


FIG. 1: (a) up-up-down-down magnetic ordering at low temperature, (b) unit cell of pyrochlore lattice, (c) crystal field splitting due to structural transition.

II. THREE-BAND HUBBARD MODEL ON THE PYROCHLORE LATTICE

The three-band Hubbard model relevant for the family of spinel vanadates AV_2O_4 is

$$\begin{aligned} \mathcal{H}_{3\text{BH}} = & - \sum_{\alpha, \sigma} \left[t_{\alpha} \sum_{\langle \mathbf{r}, \mathbf{r}' \rangle \in \alpha} \left(d_{\alpha\sigma}^{\dagger} \mathbf{r} d_{\alpha\sigma} \mathbf{r}' + \text{H.c.} \right) \right] - \sum_{\alpha} \left[\mu_{\alpha} \sum_{\mathbf{r}, \sigma} n_{\alpha\sigma} \mathbf{r} \right] \\ & + U \sum_{\mathbf{r}, \alpha} [n_{\alpha\uparrow} \mathbf{r} n_{\alpha\downarrow} \mathbf{r}] + \left(\frac{U}{2} - \frac{5J}{4} \right) \sum_{\mathbf{r}, \alpha, \beta \neq \alpha, \sigma, \sigma'} [n_{\alpha\sigma} \mathbf{r} n_{\beta\sigma'} \mathbf{r}] \\ & - \frac{J}{4} \sum_{\mathbf{r}, \alpha, \beta \neq \alpha} [\vec{\sigma}_{\alpha} \mathbf{r} \cdot \vec{\sigma}_{\beta} \mathbf{r}] + J \sum_{\mathbf{r}, \alpha, \beta \neq \alpha\sigma} \left[d_{\alpha\uparrow}^{\dagger} \mathbf{r} d_{\alpha\downarrow}^{\dagger} \mathbf{r} d_{\beta\downarrow} \mathbf{r} d_{\beta\uparrow} \mathbf{r} + \text{H.c.} \right], \end{aligned} \quad (1)$$

where the operator $d_{\alpha\sigma}^{\dagger} \mathbf{r}$ creates an electron of spin σ in the orbital α of the V^{3+} ion with coordinates \mathbf{r} , $n_{\alpha\sigma} \mathbf{r} = d_{\alpha\sigma}^{\dagger} \mathbf{r} d_{\alpha\sigma} \mathbf{r}$, and $\sigma_{\alpha}^{\delta} \mathbf{r} = \sum_{\mu, \nu} d_{\alpha\mu}^{\dagger} \mathbf{r} \sigma_{\mu\nu}^{\delta} d_{\alpha\nu} \mathbf{r}$, where σ^{δ} are the Pauli matrices. t_{α} is the transfer integral between α -orbitals of nearest-neighbor V^{3+} ions, U is the intra-orbital Coulomb repulsion, J is Hund's coupling, μ_{α} is the chemical potential whose orbital dependence is a consequence of the crystal field splitting induced by the structural transition, $\mu_{yz} = \mu_{zx} = \mu_{xy} - \Delta$, and $\sum_{\langle \mathbf{r}, \mathbf{r}' \rangle \in \alpha}$ represents summation over all pairs of the nearest-neighbor sites connected by α -type bonds. (As shown in Fig.1(b), the pyrochlore lattice has

three types of bonds: xy , yz , and zx .) This implies that electrons occupying an α -orbital can only move along the single chain of α -type bonds that contains such orbital. Note that the on-site interaction term has only two independent parameters, U and J , because of the rotational symmetry of the single-ion Hamiltonian [11].

By expanding around the strong-coupling limit of $\mathcal{H}_{3\text{BH}}$, Tsunetsugu and Motome derived an effective Kugel-Komuskii Hamiltonian whose ground state exhibits anti-ferro layered orbital ordering (OO) [6]. Moreover, by adding an antiferromagnetic exchange between third-nearest-neighbor spins, they showed that an uudd-MO is stabilized and coexists with the OO [7]. Since the OO has not been observed in any member of the AV_2O_4 family, Tchernyshyov and Maitra-Valentí proposed alternative orbital orderings [8, 9]. On the other hand, by starting from the opposite weak-coupling limit, Chern and Batista derived uudd-MO without any orbital ordering by using a mean-field theory [10]. In this paper, we show that our unbiased approach not only explains the observed magnetic ordering but also the lack of the OO in the intermediate coupling-regime relevant for the vanadium spinels.

Quantum Monte-Carlo methods for the simulation of fermionic Hamiltonians such as $\mathcal{H}_{3\text{BH}}$ typically suffer from the well-known negative sign problem introduced by the fermionic statistics and by certain off-diagonal terms. To avoid the negative sign problem we replace Heisenberg-like Hund's interaction (fifth term in Eq. (1)) by an Ising-like term because. In doing so, we are assuming that the optimal magnetic ordering of $\mathcal{H}_{3\text{BH}}$ is always collinear. In addition, we eliminate the hopping of singlet pairs between different orbitals of the same atom (sixth term in Eq. (1)) by assuming that the probability of double occupancy of a given orbital remains rather low in the intermediate-coupling regime. The resulting Hamiltonian,

$$\begin{aligned} \mathcal{H} = & - \sum_{\alpha, \sigma} \left[t_{\alpha} \sum_{\langle \mathbf{r}, \mathbf{r}' \rangle \in \alpha} \left(d_{\alpha\sigma\mathbf{r}}^{\dagger} d_{\alpha\sigma\mathbf{r}'} + \text{H.c.} \right) \right] - \sum_{\alpha} \left[\mu_{\alpha} \sum_{\mathbf{r}, \sigma} n_{\alpha\sigma\mathbf{r}} \right] \\ & + U \sum_{\mathbf{r}} [n_{\alpha\uparrow\mathbf{r}} n_{\alpha\downarrow\mathbf{r}}] + \frac{U - 2J}{2} \sum_{\mathbf{r}_{\alpha}, \beta \neq \alpha, \sigma, \sigma'} [n_{\alpha\sigma\mathbf{r}} n_{\beta\sigma'\mathbf{r}}] \\ & - \frac{J}{2} \sum_{\mathbf{r}_{\alpha}, \beta \neq \alpha, \sigma} [n_{\alpha\sigma\mathbf{r}} n_{\beta\sigma\mathbf{r}}], \end{aligned} \quad (2)$$

has only diagonal on-site interactions. Since all electrons are restricted to move along one-dimensional chains, there is no fermionic sign problem (fermions cannot be exchanged) and the only remaining challenge for efficient simulations is the the presence of geometric frustration.

III. METHOD

We apply the world-line quantum Monte-Carlo method (QMC) [12] to the Hamiltonian (2). We use a modified directed-loop algorithm for the updating procedure [13]. In this algorithm, we insert a pair of discontinuities to the world-line configuration in $(d+1)$ -dimensional space, and move one of them stochastically by updating the world-line configuration. When the discontinuity comes back to the creation point where the other discontinuity is located, these discontinuities annihilate each other. Although the Hamiltonian (2) does not cause any negative sign problem, the geometrically frustrated nature of the underlying lattice generates a “freezing problem” at low temperatures. To solve this problem, we introduce both thermal and quantum annealing in our QMC simulations. In the thermal annealing process, we start from an inverse temperature β_{init} and add $\delta\beta$ every N_{ann} Monte-Carlo sweeps. We choose $\beta_{\text{init}} = 1.0(\text{eV}^{-1})$, $N_{\text{ann}} = 300$, and $\delta\beta = (\beta - \beta_{\text{init}})/(N_{\text{change}} - 1)$ so that the inverse temperature is β after N_{change} temperature changes. Because of the rather strong interaction between electrons, the discontinuity is often geometrically trapped and localized. To avoid this “freezing of the simulation”, we apply a quantum annealing technique. We add a new term,

$$\begin{aligned} \mathcal{H}_q = -\frac{q}{2} \sum_{\mathbf{r}, \alpha, \beta \neq \alpha, \sigma, \sigma'} & \left[\left(d_{\alpha\sigma}^\dagger \mathbf{r} d_{\beta\sigma'}^\dagger \mathbf{r} + d_{\alpha\sigma}^\dagger \mathbf{r} d_{\beta\sigma'} \mathbf{r} + d_{\alpha\sigma}^\dagger \mathbf{r} d_{\beta\sigma'}^\dagger \mathbf{r} d_{\beta\sigma'} \mathbf{r} + \text{H.c.} \right) \right. \\ & \left. + d_{\alpha\sigma}^\dagger \mathbf{r} d_{\alpha\bar{\sigma}} \mathbf{r} d_{\beta\sigma'}^\dagger \mathbf{r} d_{\beta\bar{\sigma}'} \mathbf{r} \right], \end{aligned} \quad (3)$$

to \mathcal{H} to liberate the trapped discontinuity. We use the re-weighting technique to calculate the physical quantities of \mathcal{H} from the simulation with $\mathcal{H} + \mathcal{H}_q$. The procedure is rather simple. We sample the world-line configurations only without any vertices corresponding to \mathcal{H}_q . We choose q as $q\beta = 0.002 \ll 1$ so that we can sample 90% of world line configurations.

We define the unit cell of the pyrochlore lattice as shown in Fig. 1(c). The primitive vectors are $\mathbf{a}_1 = (1/2, 1/2, 0)$, $\mathbf{a}_2 = (1/2, 0, 1/2)$, and $\mathbf{a}_3 = (0, 1/2, 1/2)$. Each unit cell is labeled by $\mathbf{R} = \sum_i n_i \mathbf{a}_i$ (n_i is integer). The coordinates of the four ions in the unit cell are $\mathbf{e}_1 = (1/4, 0, 0)$, $\mathbf{e}_2 = (0, 1/4, 0)$, $\mathbf{e}_3 = (0, 0, 1/4)$, and $\mathbf{e}_4 = (1/4, 1/4, 1/4)$. To reveal the existence of udd-MO and estimate the magnetic transition temperature, we calculate the susceptibility

$$\chi_s = \frac{1}{N_{\text{site}}} \left\langle \left(\sum_{\mathbf{R}} L_{\mathbf{R}}^{(1)} \right)^2 + \left(\sum_{\mathbf{R}} L_{\mathbf{R}}^{(2)} \right)^2 \right\rangle, \quad (4)$$

where

$$L_{\mathbf{R}}^{(1)} \equiv \sum_{\alpha} \left(\sigma_{\alpha\mathbf{R}+\mathbf{e}_1}^z - \sigma_{\alpha\mathbf{R}+\mathbf{e}_2}^z + \sigma_{\alpha\mathbf{R}+\mathbf{e}_3}^z - \sigma_{\alpha\mathbf{R}+\mathbf{e}_4}^z \right),$$

$$L_{\mathbf{R}}^{(2)} \equiv \sum_{\alpha} \left(\sigma_{\alpha\mathbf{R}+\mathbf{e}_1}^z - \sigma_{\alpha\mathbf{R}+\mathbf{e}_2}^z - \sigma_{\alpha\mathbf{R}+\mathbf{e}_3}^z + \sigma_{\alpha\mathbf{R}+\mathbf{e}_4}^z \right),$$

$L_{\mathbf{R}}^{(1,2)}$ is the order parameter for uudd-MO, i.e., $\langle L_{\mathbf{R}}^{(1)} \rangle$ or $\langle L_{\mathbf{R}}^{(2)} \rangle$ is finite in uudd-MO.

IV. RESULTS

We use $U = 3.9$ (eV), and $J = 0.8$ (eV) close to the previous theoretical works [6, 9, 14]. (t is estimated as 0.35(eV) [15].) Since we are focusing on the magnetic order transition, we assume that the crystal has tetragonal symmetry: $\Delta > 0$. For concreteness, we use $\mu_{xy} = 3.05$ (eV) and $\Delta = 1.0$ (eV) so that one electron occupies xy orbital and the other electron occupies the yz or zx orbitals at low temperatures. Figure 2 shows the results of our QMC simulations at $t = 0.8$ (eV). The finite size scaling of $\chi_s L^{-2+\eta}$ has a crossing point at $T = 0.145 \pm 0.005$ (eV) where the specific heat curves have a peak. Figure 3 shows five transition temperatures estimated by using the same finite-size scaling analysis.

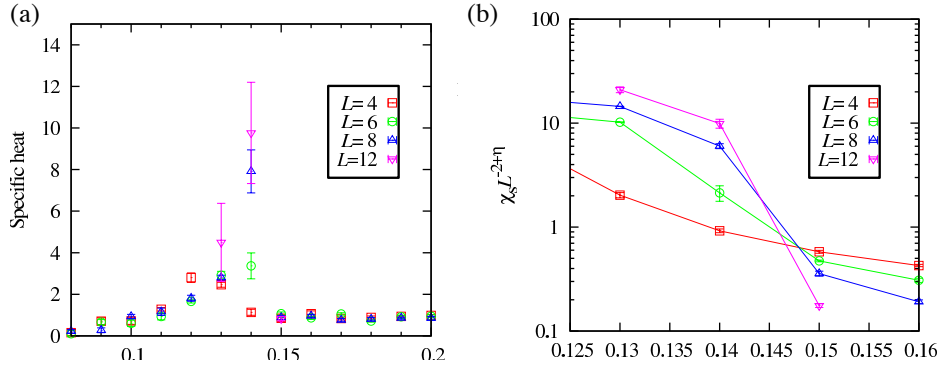


FIG. 2: Results of quantum Monte Carlo simulation with $U = 3.9$ (eV), $J = 0.8$ (eV), $\Delta = 1$ (eV), $\mu_{xy} = 3.05$ (eV), $t = 0.8$ (eV), (a) specific heat, (b) finite-size scaling of χ_s by assuming second order phase transition with 3D Z_2 symmetry breaking (i.e., $\eta = 0.04$).

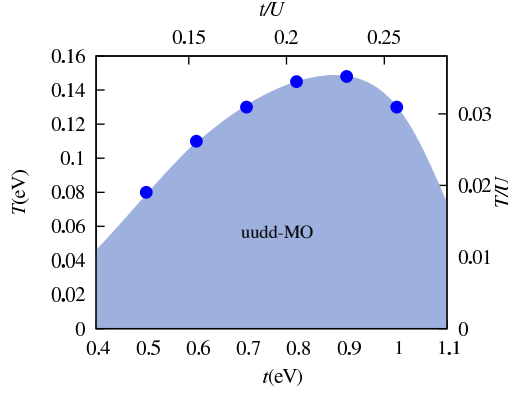


FIG. 3: Phase diagram at $U = 3.9$ (eV), $J = 0.8$ (eV), $\Delta = 1$ (eV), and $\mu_{xy} = 3.05$ (eV) with $t = t_{xy} = t_{yz} = t_{zx}$. Blue shaded regime is guide to line.

V. DISCUSSIONS AND CONCLUSIONS

The transition temperature changes non-monotonically as a function of t . By calculating

$$\chi_o = \frac{1}{N_{\text{site}}} \left\langle \left[\sum_{\mathbf{R}} \left(\Delta n_{\mathbf{R}+\mathbf{e}_1} + \Delta n_{\mathbf{R}+\mathbf{e}_2} - \Delta n_{\mathbf{R}+\mathbf{e}_3} - \Delta n_{\mathbf{R}+\mathbf{e}_4} \right) \right]^2 \right\rangle, \quad (5)$$

where $\Delta n_{\mathbf{r}} = \sum_{\sigma} n_{yz\sigma} \mathbf{r} - n_{zx\sigma} \mathbf{r}$, we have also confirmed the OO proposed by Tsunetsugu-Motome type does not appear for the range of parameters shown in Figure 3. This result is qualitatively consistent with the above mentioned experimental observations. On the other hand, the magnitude of T_N is much higher than the observed values, but it drops very rapidly for smaller values of t/U . The natural question is if the OO is still absent for values of t/U such that T_N becomes comparable to the experimental values. An answer to this question requires of very low-temperature simulations for which the freezing problem becomes more challenging. It is important to note that the rather high value of Δ that we used for our simulations tends to increase T_N because of the localization of a single electron ($S = 1/2$) in the xy -orbital. We are also ignoring the π -bond hopping of electrons that can reduce further the magnitude of T_N . Takubo *et.al* estimated the amplitude of π hopping is half of t [15].

In summary, we obtained the observed uudd-MO without OO for the intermediate-coupling regime of the three-band Hubbard model by using QMC simulations complemented by thermal and quantum annealing techniques. Preliminary results for $t = 0.3$ (eV) (not

shown in this paper) are also confirming the existence of the OO proposed by Tsunetsugu and Motome [6]. A complete the phase diagram that includes to the transition to the strong-coupling regime will be presented in a future work.

Acknowledgement

I appreciate G-W. Chern, N. Parkins, C.D. Batista for fruitful discussions. Work at the LANL was performed under the auspices of the U.S. DOE contract No. DE-AC52-06NA25396 through the LDRD program. The numerical simulations in this paper were implemented at the National Energy Research Scientific Computing Center.

-
- [1] Y. Ueda, N. Fujiwara, H. Yasuoka, Magnetic and structural transitions in $(Li_xZn_{1-x})V_2O_4$ with the spinel structure, J. Phys. Soc. Jpn. 66 (1997) 778–783.
 - [2] A. Vasiliev, M. Markina, M. Isobe, Y. Ueda, Specific heat and magnetic susceptibility of spinel compounds CdV_2O_4 , ZnV_2O_4 and $MgTi_2O_4$, Journal of Magnetism and Magnetic Materials 300 (2006) e375–e377.
 - [3] S. Nizioł, Investigation of magnetic properties of ZnV_2O_4 spinel, Physica Status Solidi (a) 18 (1973) K11–K13.
 - [4] S. Blanco-Canosa, F. Rivadulla, V. Pardo, D. Baldomir, J.-S. Zhou, M. García-Hernández, M. A. López-Quintela, J. Rivas, J. B. Goodenough, Enhanced pressure dependence of magnetic exchange in $A^{2+}[V_2]O_4$ spinels approaching the itinerant electron limit, Phys. Rev. Lett. 99 (2007) 187201.
 - [5] D. Bloch, The 103 law for the volume dependence of superexchange, Journal of Physics and Chemistry of Solids 27 (1966) 881 – 885.
 - [6] H. Tsunetsugu, Y. Motome, Magnetic transition and orbital degrees of freedom in vanadium spinels, Phys. Rev. B 68 (2003) 060405.
 - [7] Y. Motome, H. Tsunetsugu, Orbital and magnetic transitions in geometrically frustrated vanadium spinels: Monte carlo study of an effective spin-orbital-lattice coupled model, Phys. Rev. B 70 (2004) 184427.

- [8] O. Tchernyshyov, Structural, orbital, and magnetic order in vanadium spinels, Phys. Rev. Lett. 93 (2004) 157206.
- [9] T. Maitra, R. Valentí, Orbital order in ZnV_2O_4 , Phys. Rev. Lett. 99 (2007) 126401.
- [10] G. Chern, C. Batista, Spin superstructure and noncoplanar ordering in metallic pyrochlore magnets with degenerate orbitals, Phys. Rev. Lett. 107 (2011) 186403.
- [11] E. Dagotto, T. Hotta, A. Moreo, Colossal magnetoresistant materials: the key role of phase separation, Physics Reports 344 (2001) 1–153.
- [12] N. Kawashima, K. Harada, Recent developments of world-line monte carlo methods, J. Phys. Soc. Jpn. 73 (2004) 1379–1414.
- [13] Y. Kato, N. Kawashima, Quantum monte carlo method for the bose-hubbard model with harmonic confining potential, Phys. Rev. E 79 (2009) 021104.
- [14] V. Pardo, S. Blanco-Canosa, F. Rivadulla, D. Khomskii, D. Baldomir, H. Wu, J. Rivas, Homopolar bond formation in ZnV_2O_4 close to a metal-insulator transition, Phys. Rev. Lett. 101 (2008) 256403.
- [15] K. Takubo, J. Son, T. Mizokawa, H. Ueda, M. Isobe, Y. Matsushita, Y. Ueda, Electronic structure of AV_2O_4 ($A= Li, Zn, \text{ and } Cd$) studied by x-ray photoemission spectroscopy, Phys. Rev. B 74 (2006) 155103.